HNPS Advances in Nuclear Physics

Vol 29 (2023)

HNPS2022

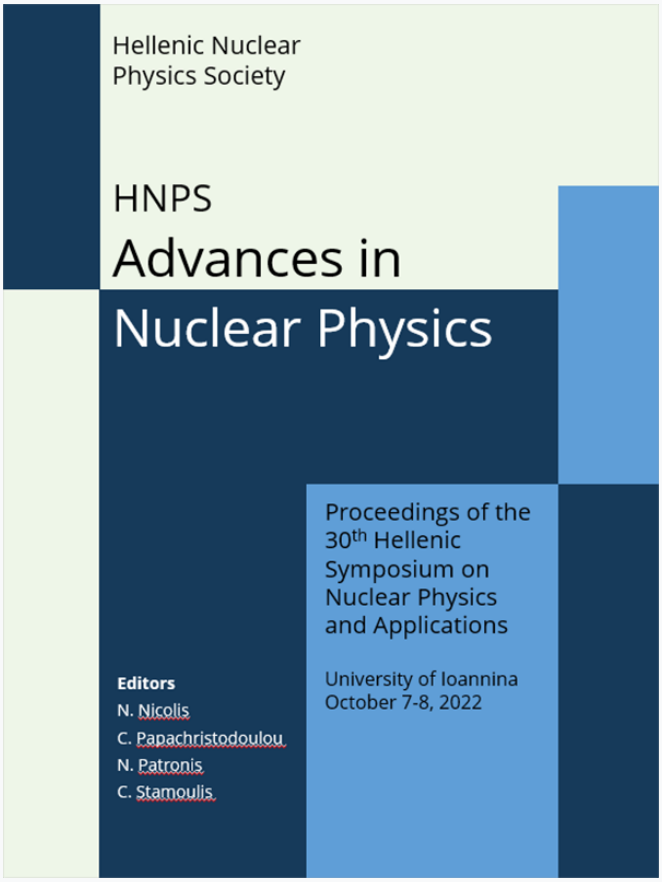

Recent Progress in the Study of the Reaction 70Zn (15 MeV/nucleon) + 64Ni with the MAGNEX Spectrometer

Stergios Koulouris, Georgios Souliotis, Francesco Cappuzzello, Diana Carbone, Athena Pakou, Clementina Agodi, Giuseppe Brischetto, Manuela Cavallaro, Salvatore Calabrese, Irene Ciraldo, Olga Fasoula, Jozef Klimo, Konstantina Palli, Onoufrios Sgouros, Vasilis Soukeras, Alessandro Spatafora, Domenico Torresi, Martin Veselsky

doi: 10.12681/hnpsanp.5090

HNPS Advances in Nuclear Physics, *29*, 45–51. https://doi.org/10.12681/hnpsanp.5090

Recent Progress in the Study of the Reaction ^{70}Zn (15 MeV/nucleon) + ^{64}Ni with the MAGNEX Spectrometer

S. Koulouris[1,*], G. A. Souliotis[1], F. Cappuzzello[2,3], D. Carbone[3], A. Pakou[4], C. Agodi[3], G. Brischetto[2,3], S. Calabrese[3], M. Cavallaro[3], I. Ciraldo[2,3], O. Fasoula[1], J. Klimo[5], K. Palli[1], O. Sgouros[3], V. Soukeras[3], A. Spatafora[2,3], D. Torresi[3], M. Veselsky[6]

[1] *Laboratory of Physical Chemistry, Department of Chemistry, National and Kapodistrian University of Athens, Athens, Greece*
[2] *Dipartimento di Fisica e Astronomia "Ettore Majorana", Universita di Catania, Italy*
[3] *Laboratori Nazionali del Sud, INFN, Catania, Italy*
[4] *Department of Physics and HINP, The University of Ioannina, Ioannina, Greece*
[5] *Institute of Physics, Slovak Academy of Sciences, Bratislava, Slovakia*
[6] *Institute of Experimental and Applied Physics, Czech Technical University, Prague, Czech Republic*

Abstract The present paper is focused on our recent efforts to study the production and identification of neutron-rich, medium-mass rare isotopes from peripheral reactions at beam energies around and below the Fermi energy. We obtained high-quality experimental data from a recent experiment with the MAGNEX spectrometer at the INFN-LNS in Catania, Italy. The main aim of this experiment was to check the feasibility of ejectile identification in this energy regime with the use of a large acceptance magnetic spectrometer. Our developed technique for particle identification depends mainly on a reconstruction of both the atomic number Z and the ionic charge q of the ions, followed by the identification of the mass. Our method was successfully applied to identify neutron-rich ejectiles from multinucleon transfer from the reaction of ^{70}Zn (15 MeV/nucleon) + ^{64}Ni. Preliminary results indicate that the extracted experimental distributions, along with comparisons with the theoretical models could help us to shed light to the complex reaction mechanism of multinucleon transfer in this energy regime.

Keywords Particle Identification, Rare Isotope Production, Magnetic Spectrometer, Multinucleon Transfer

INTRODUCTION

To date, approximately one half of the theoretically estimated 7000 bound nuclei have been produced and investigated [1]. One of the main concurrent challenges of the nuclear community in rare isotope beam facilities around the world is the production of exotic nuclides to the limit of the neutron dripline (see, e.g., [2-8]). The investigation of neutron-rich nuclei could lead to a better understanding of important astrophysical nucleosynthesis processes, such as the rapid neutron capture process (r-process), which is responsible for half of the abundance of the nuclides heavier than iron [9]. To have access to nuclides with high neutron-excess, besides the conventional routes of projectile fragmentation, fission and spallation, it is necessary to pick up neutrons from the target [10]. Such nucleon transfer mechanisms mainly take place in peripheral nucleon-exchange reactions at beam energies from the Coulomb barrier to the Fermi energy (~15-20 MeV/nucleon) [11, 12]. The main interest of our research group is the study of heavy-ion reactions well above the Coulomb barrier, but below the Fermi Energy in order to access nuclides with high neutron excess [13-18]. However, for the efficient collection of these fragments, the use of a large acceptance spectrometer is essential. For this reason, we initiated a project to produce and identify projectile-like fragments with the MAGNEX large-acceptance spectrometer at the INFN-LNS from the reaction ^{70}Zn^{15+} (15 MeV/nucleon) + ^{64}Ni. This project is a first experiment, aiming to check the feasibility of ejectile identification in this energy regime with the use of a large acceptance magnetic spectrometer.

* Corresponding author: stekoul@chem.uoa.gr

EXPERIMENTAL DETAILS

The measurements took place at the MAGNEX facility of the Istituto Nazionale di Fisica Nucleare, Laboratori Nazionali del Sud (INFN-LNS) in Catania, Italy. MAGNEX is a large-acceptance magnetic spectrometer installed at the INFN-LNS laboratory in Catania, Italy. It is a high-acceptance device which utilizes both the advantages of the traditional magnetic spectrometry and those of a large momentum and angular acceptance detector [19-21]. A beam of $^{70}Zn^{15+}$ at 15 MeV/nucleon delivered by the K800 superconducting cyclotron bombarded a 1.18 mg/cm^2 ^{64}Ni foil. The ejectiles emerging from the target passed through a 6 μm Mylar stripper foil, in order to reset their charge state to the equilibrium charge state value (+29) and then were momentum analyzed by the MAGNEX spectrometer and detected by its focal plane detector (FPD) [22, 23].

The focal plane detector (FPD) is a large (1360×200×90 mm^3 active volume) gas-filled hybrid detector with a wall of 60 large-area silicon detectors (50×70×0.5 mm^3) arranged in three rows at the end. It mainly consists of two parts: a gas tracker sensitive to the energy loss of the reaction products and a stopping wall of silicon detectors for the measurement of their residual energy. The detector mainly consists of a Mylar foil (6 μm) at the entrance window and a proportional drift chamber spanning at six sequential planes, responsible for the extraction of the horizontal and vertical coordinates of each incident particle, thus, leading to a simultaneous determination of the angles theta (θ) and phi (φ) of the ion's trajectory. Moreover, the FPD provides the energy loss of the reaction products in the gas and the residual energy of these fragments in the silicon detectors. Finally, the time-of-flight (TOF) of the ions was measured via a start signal from the silicon detectors of FPD and a stop signal from the radiofrequency of the cyclotron.

In the present experiment, only about one-half of the active area of FPD was used (the other part was covered with an aluminum screen) in order to avoid radiation damage of the silicon detectors and high dead times due to limitations in the data acquisition system. These experimental restrictions will be circumvented in the future in view of the upgrading of the MAGNEX facility. The restriction of the vertical acceptance and the active area of the FPD resulted in the use of only seven of the silicon detectors of the FPD.

PARTICLE IDENTIFICATION PROCEDURE

The particle identification procedure is based on a novel approach that we developed in [24] and is influenced by the procedure presented in [23]. The determination of the atomic number of the ejectiles involves a correlation between the residual energy measured by the silicon detectors (E_{resid}) and the total energy loss (ΔE_{cor}) in the gas section of the FPD corrected for path length differences depending on the angle of incidence. In Fig. 1, we present two plots depicting the total energy loss at the gas section of the FPD vs the residual energy measured by a single silicon detector. On the left-hand side, we present the results of our data from the reaction of ^{70}Zn + ^{64}Ni with the MAGNEX spectrometer. In the plot on the right, we can see the results from the analysis that was carried out in [25]. It is evident that this correlation is quite useful for the determination of the atomic number Z in light ions. However, in our case of heavier medium-mass ions, we could not obtain an effective Z separation.

Based on this observation we moved on to a systematic approach to reconstruct the atomic number Z, by making use of the measured and calibrated quantities ΔE_{cor}, E_{resid} and TOF. Guided by Bethe's stopping power formula $\Delta E \propto \frac{Z^2}{v^2}$, Z is reconstructed according to the following expression:

$$Z = a_0(v) + a_1(v) v\sqrt{\Delta E_{cor}} + a_2(v)(v\sqrt{\Delta E_{cor}})^2 . \quad (1)$$

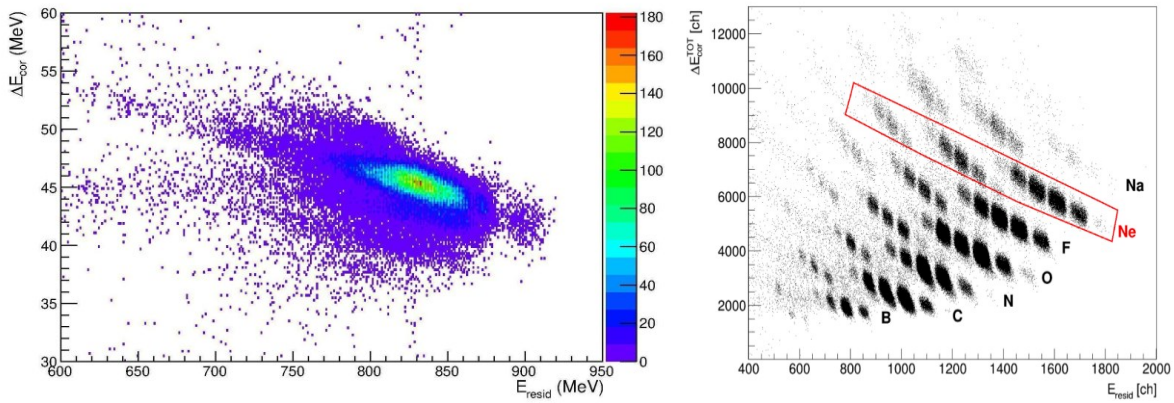

Figure 1. *ΔE_{cor} vs E_{resid} correlation for the identification of Z. On the left, our data from the reaction of ^{70}Zn + ^{64}Ni with the MAGNEX spectrometer are presented. On the right, data from [20] for $^{20}Ne^{10+}$ induced reactions are presented.*

In order to determine the functions $a_0(\upsilon)$, $a_1(\upsilon)$ and $a_2(\upsilon)$ in the velocity range of interest, we used the energy-loss data of Hubert et al. [26] to determine the coefficients of this equation for the Z range 6-36 and in the energy range 8-18 MeV/nucleon by applying a least-squares fitting procedure at each energy in steps of 0.5 MeV/nucleon. The values of each coefficient at the various energies were then fitted with polynomial functions of velocity.

The TOF measurement, along with the trajectory length of each particle, led to the calculation of the ionic charge state from the equation:

$$q = \frac{2\,E_{tot}}{B\,\rho}\,\frac{L}{TOF}\,, \tag{2}$$

where L is the trajectory length obtained from the trajectory reconstruction procedure, Bρ the magnetic rigidity and E_{tot} is the total kinetic energy of the ions reaching the FPD and determined from the expression:

$$E_{tot} = \Delta E_{tot} + \Delta E_w + E_{resid}\,, \tag{3}$$

where ΔE_{tot} is the sum of the measured energy loss in the gas section of the FPD, E_{resid} the residual energy measured by the Si detectors and ΔE_w a calculated correction for the energy loss in the entrance window of the FPD. The magnetic rigidity is obtained from the following equation:

$$B\rho = B\rho_0\,(1 + \delta), \tag{4}$$

with $B\rho_0$ being the magnetic rigidity of the central trajectory and δ the fractional deviation from central trajectory, derived from the standard procedure of optical reconstruction of MAGNEX [13, 14].

Our effort for particle identification involves a correlation of the reconstructed atomic number Z with the reconstructed ionic charge state q of the products in a two-dimensional plot. We were in position to select events of specific Z and q after proper gating. An example of this approach can be found in [24, 27, 28].

We will now focus on the procedure of mass identification after the reconstruction of the atomic number Z and the charge state q. For the determination of the masses, we have set gates on Z and q for each Si detector. After proper gating, we implement the standard approach of mass identification for large acceptance spectrometers. This is mainly based on the relationship between the total kinetic energy of the ions and the magnetic rigidity which can be expressed as:

$$B\rho = \frac{\sqrt{m}}{q}\,\sqrt{2\,E_{tot}}\,. \tag{5}$$

We can see that this equation expresses a proportionality of the magnetic rigidity on $\sqrt{E_{tot}}$ with a slope of $\sqrt{m}/q$. Thus, a correlation of Bρ on $\sqrt{E_{tot}}$ or, (for simplicity) on E_{tot} should result on a grouping of the particles in bands of the same $\sqrt{m}/q$. But since in our procedure we have fixed q, the bands should correspond to successive masses. It is also important to notice that the magnetic rigidity

is mainly determined by the position at the focal plane of the spectrometer and since only a small fraction of the energy is deposited in the gas, the above relationship is approximately maintained between the two primary measured quantities X_{foc} and E_{resid}, where these two quantities provide the basis of the mass identification.

In Fig. 2, we present a Bρ versus E_{tot} plot of the Zn^{28+} (Z=30, q=28) of events for a single Si detector. In this representation, the selection of the various masses can be performed by setting the respective graphical cuts, as shown for A = 68–72 in the case of Zn^{28+} ejectiles.

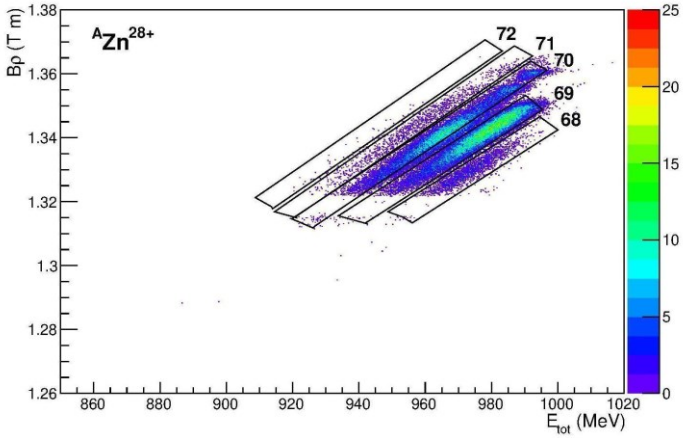

Figure 2. *Magnetic rigidity vs total energy correlation of ejectiles with Z = 30 and Q = 28 from the reaction ^{70}Zn (15 MeV/nucleon) + ^{64}Ni. The graphical contours represent isotopes of Zn^{28+} (A = 68-72).*

The next step of our analysis is the extraction of momentum spectra, angular distributions and production cross sections. After setting proper graphical cuts in the Bρ versus E_{tot} plot, we manually save these cuts for further use. We note that each cut at this point represents an ejectile of specific Z, Q and A. Having determined the isotopes of each Si detector, for each Z, Q, A we proceed to a new correlation and that is a reaction angle versus magnetic rigidity as can be seen in Fig. 3. Each channel of this plot (events of a given reaction angle, theta, and Bρ and their respective counts), is stored properly and used as input for an appropriate data manipulation program developed in our lab. This program is responsible for constructing a multidimensional distribution that yields the cross section as a function of Z, A, theta and momentum per nucleon (P/A), leading ultimately to mass, angular and momentum per nucleon distributions as can be seen in the next section where we present our first experimental results.

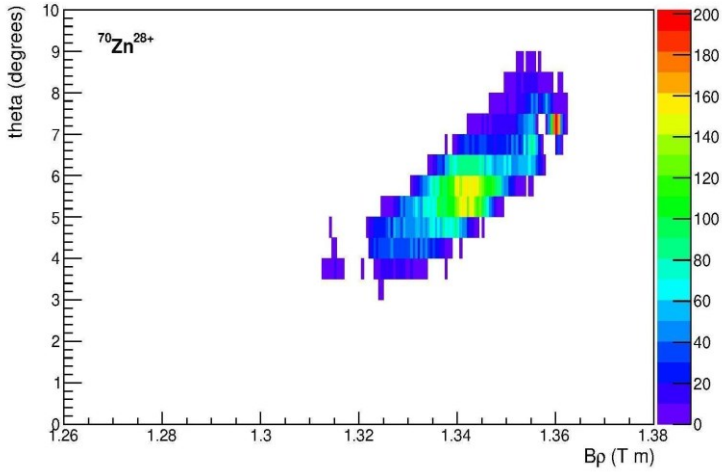

Figure 3. *Reaction angle (theta) versus magnetic rigidity (Bρ) of ejectiles with Z = 30 and Q = 28, A = 70 for one Si detector from the reaction ^{70}Zn (15 MeV/nucleon) + ^{64}Ni*

EXPERIMENTAL RESULTS

The observable of momentum per nucleon (P/A), namely the velocity of the particles, is a measure of the energy dissipation caused by the interaction of the projectile-target binary system, and thus can provide important information on the mechanism responsible for the production of the fragments of interest. The general feature of the momentum distributions, as expected, is the presence of two main regions: a) a quasielastic peak that corresponds to direct processes, and b) a broad region, located at lower values of P/A that corresponds to deep inelastic processes involving extensive multinucleon transfers. The general feature of angular distributions is that they peak near the grazing angle. However, elements further away from the projectile are characterized by a rather monotonically decreasing angular distribution. In Fig. 4 we present our first experimental angular and momentum per nucleon distributions depicting the stripping of a neutron, the inelastic channel (^{70}Zn) and the products of the pickup of one and two neutrons from the target. The data are shown by solid black circles. The green

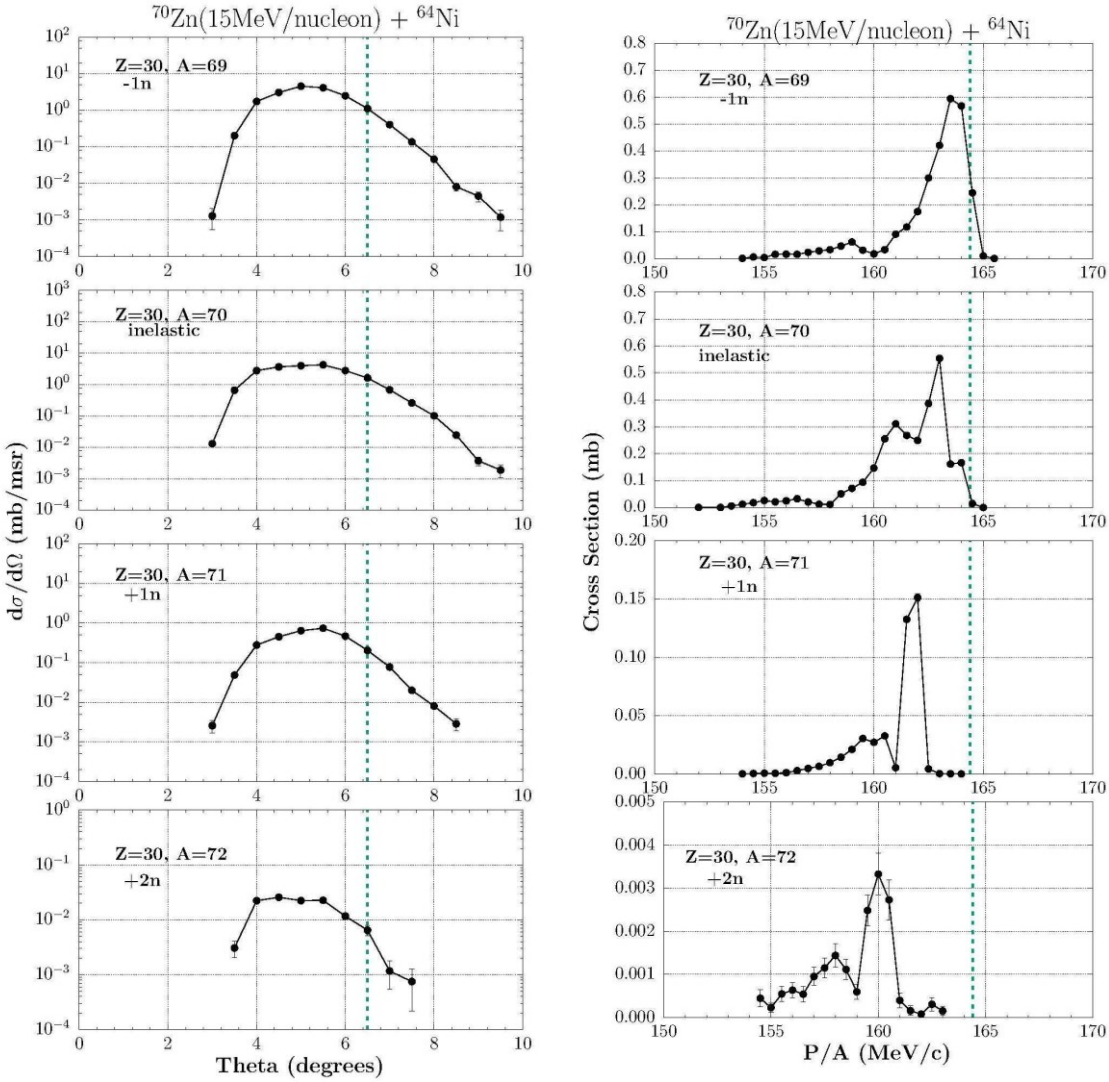

Figure 4. *Angular (left-hand side) and P/A (right-hand side) distributions (differential cross sections) of projectile fragments from the reaction of ^{70}Zn (15 MeV/nucleon) + ^{64}Ni. Experimental data (closed black circles) of the channels of the stripping of a neutron, the inelastic channel (^{70}Zn) and the products of the pickup of one and two neutrons from the target are shown. The green vertical line indicates the grazing angle (θ_{gr} = 6.5°) of the reaction under study, while in the case of the P/A distributions, it represents the momentum per nucleon of the beam, which is 164.4 MeV/c.*

dashed line shown on each frame of the momentum distribution plot represents the momentum per nucleon of the beam, which is 164.4 MeV/c, while on the angular distribution plot represents the grazing angle of the reaction under study that is $\theta_{gr} = 6.5^{o}$.

In the following P/A distribution, we can clearly see a gradual shift towards lower values of P/A. This is due to the fact that the pickup of more nucleons from the projectile, indicates a longer interaction between the projectile-target binary system, ultimately leading to a stronger dissipation and thus to lower values of momentum per nucleon. It is also very interesting to notice that in the two-neutron pickup channel a dense broad region can be found in lower values of P/A. It is a strong indication of the complex mechanisms that could possibly lead to this neutron-rich product.

In Fig. 5, we present the extracted production cross sections for each isotope of the elements with Z = 27–32 from the reaction of ^{70}Zn (15 MeV/nucleon) with ^{64}Ni. Solid black circles correspond to the experimental data. In this figure, we also show the calculated mass distributions of projectile fragments with Z = 27–32 from the same reaction obtained by the DIT/GEMINI codes (dashed red line with closed circles). The vertical dashed green line indicates the starting point of neutron pickup. In this figure we can make some interesting remarks. First of all, for elements close to the projectile (e.g., for Z =30) we can see the pickup of up to three neutrons, as well as in the case of Ge (Z = 32) where the pickup goes up to two neutrons. Interestingly, it seems that the phenomenological DIT model seems to agree with the experimental data on the neutron-rich side of the yield distributions. However, we see that there is a disagreement between the calculations and the data for the case of elements further away from the projectile, as in the case of Co (Z = 27) and Ni (Z = 28). The reason of this discrepancy seems to be the

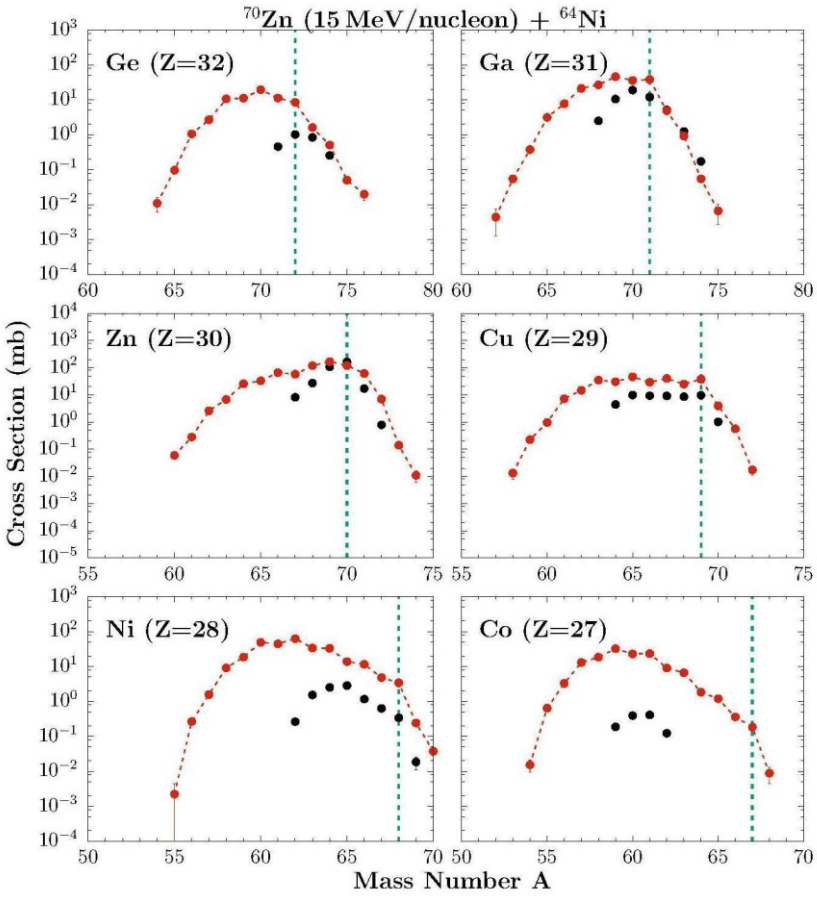

Figure 5. *Experimental mass distributions of projectile-like fragments from the reaction of ^{70}Zn (15 MeV/nucleon) + ^{64}Ni. The experimental data are shown by solid black points. The DIT/GEMINI calculation is shown with a dashed red line with closed red circles. The vertical dashed green line shows the beginning of neutron pick-up.*

Bρ coverage during this experiment. We note that in this exploratory run the Bρ range was not covered adequately for the complete collection of these ejectiles, as we focused on neutron-rich fragments very close to the projectile.

CONCLUSIONS

In the present work, the MAGNEX spectrometer was used to identify medium-mass ejectiles from the reaction of a ^{70}Zn beam at 15 MeV/nucleon energy with a ^{64}Ni target. For the analysis of the data, we developed a systematic approach to reconstruct both the atomic number Z and the ionic charge state q. Then, for each Si detector used, we moved on to a correlation of the reconstructed atomic number and the measured charge states to identify particles of specific Z and Q. Finally, a correlation of the magnetic rigidity versus the total energy gave us a separation of masses of the isotopes. Then, through the reaction angle (theta) versus Bρ correlation we obtained important momentum, angular and mass distributions.

We have successfully obtained angular, P/A as well as cross section distributions for channels such as those of neutron pickup, proton removal and of isobaric charge exchange reactions that yield medium-mass neutron rich nuclei. We are currently trying to understand these complex distributions through comparisons of the data with theoretical model calculations such as the phenomenological DIT model [29], the microscopic CoMD [30,31], along with the statistical deexcitation code GEMINI [32] that are now underway.

References

[1] G.G. Adamian et al., Eur. Phys. J. A 56, 47 (2020)
[2] FRIB main page: www.frib.msu.edu
[3] GANIL main page: www.ganil.fr
[4] GSI main page: www.gsi.de
[5] RIBF: www.nishina.riken.jp/facility/RIBFabout_e.html
[6] ATLAS: www.phy.anl.gov/atlas/facility/index.html
[7] INFN/LNS main page: www.lns.infn.it
[8] RISP main page: www.risp.re.kr/eng/pMainPage.do
[9] H. Grawe et al., Rep. Prog. Phys. 70, 1525 (2007)
[10] Y.X Watanabe et al., Phys. Rev. Lett. 115, 172503 (2015)
[11] T. Mijatovic, Front. Phys. 10:965198 (2022)
[12] L. Corradi et al., J. Phys. G: Nucl. Part. Phys. 36:113101 (2009)
[13] G. A. Souliotis et al., Phys. Lett. B 543, 163 (2002)
[14] G. A. Souliotis et al., Phys. Rev. C 84, 064607 (2011)
[15] P.N. Fountas, G.A. Souliotis, M. Veselsky and A. Bonasera, Phys. Rev. C 90, 064613 (2014)
[16] A. Papageorgiou, G.A. Souliotis et al., J. Phys. G 45, 095105 (2018)
[17] O. Fasoula. G.A. Souliotis et al., HNPS Adv. Nucl. Phys. 28, 47 (2022)
[18] K. Palli, G.A. Souliotis et al., EPJ Web of Conferences 252, 07002 (2021)
[19] F. Cappuzzello et al., Eur. Phys. J. A 52, 167 (2016)
[20] F. Cappuzzello et al., Nucl. Instr. and Meth. A 621, 419 (2010)
[21] A. Cunsolo et al., Nucl. Instr. and Meth. A 481, 48 (2002)
[22] M. Cavallaro et al., Eur. Phys. J. A 48, 59 (2012)
[23] D. Torresi et al., Nucl. Instr. and Meth. A 989, 164918 (2021)
[24] G.A. Souliotis, S. Koulouris et al., Nucl. Instr. and Meth. A 1031, 166588 (2022)
[25] M. Cavallaro et al., Nucl. Instr. and Meth. B 463, 334 (2020)
[26] F. Hubert, R. Bimbot and H. Gauvin, Atom. Data and Nucl. Data Tables 46, 1 (1990)
[27] S. Koulouris, G.A. Souliotis et al., EPJ Web of Conferences 252, 07005 (2021)
[28] S. Koulouris, G.A Souliotis et al., HNPS Adv. Nucl. Phys. 28, 42 (2022)
[29] L. Tassan-Got and C. Stephan, Nucl. Phys. A 524, 121 (1991)
[30] M. Papa et al., Phys. Rev. C 64, 024612 (2001)
[31] M. Papa et al., J. Comput. Phys. 208, 403 (2005)
[32] R. Charity et al., Nucl. Phys. A 483, 371 (1988)